

Supplementary Materials for

Donor pulmonary intravascular nonclassical monocytes recruit recipient neutrophils and mediate primary lung allograft dysfunction

Zhikun Zheng, Stephen Chiu, Mahzad Akbarpour, Haiying Sun, Paul A. Reyfman, Kishore R. Anekalla, Hiam Abdala-Valencia, Daphne Edgren, Wenjun Li, Daniel Kreisel, Farida V. Korobova, Ramiro Fernandez, Alexandra McQuattie-Pimentel, Zheng J. Zhang, Harris Perlman, Alexander V. Misharin, G. R. Scott Budinger, Ankit Bharat*

*Corresponding author. Email: abharat@nm.org

Published 14 June 2017, *Sci. Transl. Med.* **9**, eaal4508 (2017)

DOI: 10.1126/scitranslmed.aal4508

The PDF file includes:

Materials and Methods

Fig. S1. Cytokine analysis of the lung allograft.

Fig. S2. Representative gating strategy to evaluate the myeloid cell populations in the lungs.

Fig. S3. Perfusion of the heart-lung block.

Fig. S4. Effects of monocyte depletion strategies on the donor.

Fig. S5. Effects of donor clo-lip treatment on the 24-hour posttransplant allograft.

Fig. S6. Donor clo-lip treatment abrogates neutrophil influx after syngeneic lung transplant.

Fig. S7. Effects of CX3CR1 deletion on nonmonocyte cell populations in the lung and blood and on the posttransplant allograft.

Fig. S8. Effects of NR4A1 deletion on non-monocyte cell populations in the lung and blood and on the posttransplant allograft.

Fig. S9. All neutrophils were of recipient origin after 24 hours of reperfusion in the allograft.

Fig. S10. Representative gating strategy of GFP-expressing cells in the lungs of *Cx3cr1^{gfp/+}* and *Cx3cr1^{gfp/gfp}* mice.

Fig. S11. NCMs do not differentiate upon lipopolysaccharide challenge.

Fig. S12. Immunofluorescence microscopy of human lung biopsy from a patient experiencing PGD.

Fig. S13. Schematic to illustrate the role of pulmonary intravascular NCMs in mediating neutrophil infiltration and lung allograft injury.

Legend for table S1

Legends for movies S1 and S2

References (52–57)

Other Supplementary Material for this manuscript includes the following:

(available at

www.sciencetranslationalmedicine.org/cgi/content/full/9/394/eaal4508/DC1)

Table S1 (Microsoft Excel format). Primary data.

Movie S1 (.mov format). PBS-lip-treated control mice reveal profound neutrophil infiltration into the lung allograft after reperfusion.

Movie S2 (.mov format). Intravenous clo-lip treatment of the donors abrogates neutrophil infiltration into the allograft after reperfusion.

SUPPLEMENTARY MATERIALS

Materials and Methods

Animals and Reagents

The mice used were 10-16 weeks and weighed 24-30 g. Wild type C57BL/6 (B6), BALB/c (B/c), *Cx3cr1^{gfp/gfp}*, *Nr4a1^{-/-}*, congenic CD45.1 and CD45.2 mice were commercially acquired (Jackson Laboratories). *Myd88^{-/-}* and *Trif^{-/-}* mice were crossed to develop *Myd88/Trif^{-/-}* mice on the B6 background. The mice were housed at Northwestern University Animal Care center, in a specific pathogen-free environment with climate controlled rooms and free access to standard pelleted food and water. All experiments using mice were performed in accordance with protocols that were approved by Northwestern University Institutional Care and Use Committee. Clodronate-loaded liposomes and control phosphate-buffered saline liposomes were purchased (Clodroliposomes). At specific time points as discussed in the results, mice were injected intravenously with 200ul of clodronate-loaded liposomes or control PBS-loaded liposomes (25). Cytotoxic anti-CCR2 antibodies were a kind gift of Steffen Jung and used for selective depletion of CCR2⁺ classical monocytes as previously described (45). Purified anti-CXCL2 antibodies (R&D Systems) and anti-CX3CR1 antibodies (Torrey Pines Biolabs) were commercially acquired. Multiplex cytokine arrays were performed according to standardized manufacturer's instructions (Luminex Multiplex Assays, ThermoFisher Scientific).

Human Donor Lungs

Lungs for human transplantation were obtained from donors who met standard donation criteria (52). The lungs were procured in a standardized fashion by first perfusing the main pulmonary artery with a low-potassium dextran (Perfadex) solution cooled to 4°C (XVIVO Perfusion) at a

volume of 60ml/kg (53). Additionally, the lungs were perfused in a retrograde manner with 250ml of the same solution through each of the four pulmonary veins. The lungs were transported for transplantation at 4°C. A 1x1 cm piece of lingula or right middle lobe was serially resected immediately after removing the lungs from cold storage, and 90 minutes following reperfusion. To achieve consistency, the serial biopsies of human lungs were obtained from the exact same region of the donor pre- and post-reperfusion. Lung specimens were processed immediately as recently described (22). Since alveolar macrophages are the most consistent cell population throughout the lung before and after transplantation (54), cell counts were expressed as a ratio per AM to achieve meaningful comparison. Human lung samples were acquired in concordance with the Northwestern University Institutional Review Board policies and regulations.

Murine lung transplantation

Orthotopic murine left lung transplantation was performed as previously described (27, 55). Donor mice were anesthetized with a mixture of xylazine (10 mg/ kg) and ketamine (100 mg/kg). The donor lungs were flushed with 3 ml of preservative solution through the pulmonary artery. The heart-lung block was excised and then stored in cooled (4°C) preservative solution. The bronchus, pulmonary vein, and artery were dissected free and prepared for anastomosis. A customized cuff made of a Teflon intravenous catheter applied to the vascular structures and fixated with a 10-0 nylon ligature. After placement of a microvessel clip on the bronchus to avoid airway infiltration with preservative solution, the graft was stored at 4°C for a period of 90-120 minutes of cold ischemic time prior to implantation. The recipient mice received subcutaneous buprenorphine (0.1 mg/kg) 30 min prior to incision and every 6 hours as needed after the procedure. The recipient mice were intubated and a left-sided thoracotomy was

performed within the third intercostal space. The recipient's native lung was gently clamped and pulled out of the thoracic cavity. The space between the artery, the vein and the bronchus was dissected separately. The artery and vein were temporarily occluded using 8-0 nylon ligatures. The anastomoses were completed by fixating each cuff with 10-0 nylon ligatures. The occlusion ligatures were released (first vein, then artery) and the lung inflated. The chest incision was closed and recipients separated from the ventilator when spontaneous respiration resumed. No antibiotics or immunosuppressive agents were used postoperatively in any groups unless otherwise noted. For reconstitution of clodronate-loaded liposome treated donors, we used 5×10^5 freshly sorted lung NCM from either wild type or *Myd88/Trif*^{-/-} mice. These NCM were injected into the pulmonary artery of the donor murine lungs *ex vivo*, immediately prior to implantation of the donor lung. For reconstitution of *Nr4a1*^{-/-} mice, freshly sorted NCM from *Cx3cr1*^{gfp/+} mice were used and injected intravenously through a retro-orbital injection.

Assessment of Lung injury

To obtain arterial oxygenation measurements, mice were intubated, mechanically ventilated on 100% oxygen, and a sternotomy was performed. The right lung hilum was clamped for 5 minutes, then 100ul of arterial blood was drawn from the aorta via a heparinized syringe and immediately analyzed using an i-STAT blood gas analyzer (Abbott). Graft function was expressed as the partial pressure of arterial oxygen (PaO₂) while on 100% inhaled oxygen (FiO₂). For histological analyses, the whole lung was harvested and gently flushed through the pulmonary artery with 3ml saline. 4% paraformaldehyde was instilled into the trachea with a pressure of 10cmH₂O then fixed for 48-72 hours prior to being embedded in paraffin. The whole

lung was serially sectioned and stained with hematoxylin and eosin (H&E). Evans blue dye extravasation and wet-dry ratio of the lungs were performed as previously described (29).

Multicolor flow cytometry

Single cell suspensions from mouse whole lung and human lung wedge biopsies were obtained as previously described (22, 56). Murine peripheral blood was storage in EDTA-coated tubes. Whole blood was utilized for staining, after which simultaneous cell fixation and red blood cell lysis was performed utilizing FACSlyse (BD Biosciences). Antibodies utilized for murine cell staining included rat-anti mouse CD24-BUV395 (M1/69, BD), rat anti-mouse CD45-FITC (30-F11, BioLegend), CD45.1-FITC (A20, BD), rat anti-mouse CD11b-FITC (M1/70, BD), rat anti-mouse I-A/I-E-FITC (M5/114.15.2, BioLegend), rat anti-mouse Ly6C-eFluor450 (HK1.4, eBiosciences), rat anti-mouse I-A/I-E-PerCPCy5.5 (M5/114.15.2, BioLegend), rat anti-mouse CD24-APC (M1/69, eBiosciences), rat anti-mouse CD45-APC (30-F11, BioLegend), rat anti-mouse CD45.2-APC (104, BD) rat anti-mouse CD3-APC (145-2C11, eBiosciences), rat anti-mouse Ly6G-AlexaFluor 700 (1A8, BioLegend), rat anti-mouse NK1.1-AlexaFluor 700 (PK136, BD), rat anti-mouse CD11b-APCCy7 (M1/70, BioLegend), rat anti-mouse CD64-PE (X54-5/7.1, BioLegend), rat anti-mouse CD115-PE (AFS98, eBiosciences), rat anti-mouse SiglecF-PECF594 (E50-2440, BD), rat anti-mouse CD19-PECF594, (1D3, BD), rat anti-mouse F4/80-APC (BM8, eBiosciences), rat anti-mouse CD11c-PECy7 (HL3, BD), rat anti-mouse CD62L-PECy7 (MEL-14, eBiosciences).

Antibodies utilized for human cell staining included mouse-anti human CD45-BB515 (HI30, BD), mouse-anti human CD14-PerCPCy5.5 (M5E2, BD), mouse anti-human HLA-DR-

eFluor450 (L243, eBioscience), mouse anti-human CD169-APC (7-239, Biolegend), mouse anti-human CD15-AlexaFluor 700 (W6D3, Biolegend), rat anti-mouse/human CD11b-APCCy7 (M1/70, Biolegend), mouse anti-human CD16-PE (3G8, BD), mouse anti-human CD163-PECF594 (GHI/61, BD), mouse anti-human CD206-PECy7 (19.2, eBioscience). Fixed samples were run on a custom LSRFortessa Cell Analyzer (BD) for flow cytometry analysis. Fresh samples were sorted using a FACS Aria (BD). Acquired data was analyzed with FlowJo v10 (FlowJo).

Two-photon Microscopy

For imaging of fresh lung explants, 100ul of a 1:4 dilution of Qtracker 655 vascular (Life Technologies) was injected intravenously and allowed to circulate for 3 minutes prior to sacrifice. Following animal sacrifice, tracheostomy was performed and the anterior chest wall was removed. 1mL of 30% sucrose was instilled via the tracheostomy, then and the right and left hila were ligated with silk suture and hilar structures transected proximal to the suture ligature. The resulting lung block thus retained alveolar inflation and contained Qtracker655 to label blood vessels. This lung block was then attached to the underside of a microscope slide cover utilizing a ring of VetBond (3M) and immersed in ice cold sterile PBS. Imaging was performed utilizing a water immersion lens on an A1R-MP+ multiphoton microscope system with a Coherent Ti:S Chameleon Vision S laser tuned to 890nm. The post-transplant intravital two-photon microscopy was performed as previously described in our previous report (11).

Immuno-Electron Microscopy

After exposing the heart and bilateral lungs, the intrathoracic inferior vena cava and aorta were transected. The right ventricle was flushed with 5mL of HBSS, followed by 5mL of fixative composed of 4% paraformaldehyde and 0.1% glutaraldehyde on 0.1 M cacodylate buffer. The bilateral lung block was then gently instilled with 1mL of fixative solution to re-recruit the alveoli and fixed in 10mL of fixative buffer overnight at 4°C. After overnight fixation, the pleura was stripped and the subpleural parenchyma minced gently into 1-2mm pieces and replaced in fixative buffer and kept at 4°C. After dehydration in a graded series of ethanol, the pieces were embedded in LRWhite embedding medium (EMS) cured at 58°C overnight. Ultra-thin sections were collected on nickel grids and were blocked with 1% BSA in PBS and primary staining performed with a 1:20 dilution of polyclonal rabbit anti-GFP (ab6556, Abcam) followed by 10 nm immunogold goat anti-rabbit IgG (Jackson Immunoresearch). The grids were contrasted with 3% aqueous uranyl acetate and Reynold's lead citrate solutions and dried. Sorted cells were fixed in the same fixative and mixed with 10% gelatin, then post-fixed with 1% osmium tetroxide, dehydrated in a graded series of ethanol and embedded in Epon812 (EMS). Ultrathin sections of cells were also contrasted with 3% aqueous uranyl acetate solution and Reynold's lead citrate, and dried. Samples were imaged using a FEI Tecnai Spirit G2 transmission electron microscope (FEI Company) operated at 80 kV. Images were captured by Eagle 4k HR 200kV CCD camera.

Compartmental Lung Intravenous and Intratracheal Staining

Intravenous and intratracheal was performed utilizing an adaptation of previously described methods (34). 6ug of APC-conjugated anti-CD45 in 100ul of sterile PBS was injected IV and allowed to circulate for 3 minutes prior to euthanasia with an overdose of Euthasol.

Tracheostomy was performed. The vena cava was transected and the right ventricle flushed with 10mL of HBSS to wash unbound IV antibody. The heart was removed and the bilateral lung block was then gently instilled with 1ug of FITC-conjugated anti-CD45 mAb in 1mL of HBSS and incubated at room temperature for 5 minutes. The instilled antibody-containing volume was then removed and 3 sequential 1mL bronchoalveolar lavage (BAL) washes were performed and collected to remove any unbound IT antibody prior to enzymatic digestion and mechanical dissociation of the whole lung. The collected BAL was washed with 10mL of MACS buffer, pelleted, re-suspended, and passed through a 40um filter and combined with the single cell suspension from the whole lung digest to proceed with ex vivo staining.

RNA sequencing

NCM were sorted from naïve, 2 hour, and 24 hour post-perfusion *Cx3cr1^{gfp/+}* lungs according to the gating strategy shown in Figure 6B. Samples with less than 10,000 cells were sorted directly into extraction buffer then thoroughly mixed. Total RNA was extracted using the Arcturus PicoPure RNA Isolation Kit (ThermoFisher) with an average yield of 18ng per naïve sample and 2.8ng per post-perfusion sample. Total RNA with an RIN>7.0 (average 8.7) was then preamplified and cDNA synthesis was performed using the SMART-Seq v4 Ultra Low Input RNA Kit for Sequencing (Clontech, Takara Bio USA). Libraries were then prepared using the Nextera XT DNA Library Preparation Kit (Illumina), indexed using the Nextera Index Kit v2 (Illumina), and sequenced on a NextSeq500 (Illumina). FASTQ files were generated, then single-end reads mapped to the mouse reference genome mm10 using TopHat2 aligner software with the HTSeq package resulting in an average of 74.7% (range 72.6-77.4%) singly-mapped reads per sample and an average of 18.5×10^6 (range $10.1-29.4 \times 10^6$) singly-mapped reads per

sample. Raw counts were used for a differential gene expression analysis using edgeR (R version 3.2.3) with an adjusted $p < 0.05$ by pair-wise comparisons to identify differentially expressed genes (DEG). A filter for genes having a count per million (cpm) sum of at least 2 including samples with at least 1cpm was done to eliminate low expressing and non-expressing genes before DEG analysis. Principle component analysis (PCA) of samples was done using \log_2 CPM (count per million reads) values of all detected genes in R. Heat maps were generated using K-means clustering with $K=3$ using GENE-E (Broad Institute), gene ontology analysis was performed using Gorilla Gene Ontology (57), and pathway analysis done using KEGG Pathways (www.kegg.jp/kegg/pathway.html).

MIP-2 analysis

Total RNA was extracted from sorted cells or pulmonary vein blood with Trizol reagent following the manufacturer's instructions (Invitrogen). cDNA was generated from 1ug RNA using superscript III reverse transcriptase (Invitrogen) following the manufacturer's instruction. Real-time PCR amplification and analysis was used the 7900HT real-time PCR system (Applied Biosystems). The relative amount of gene was normalized to B-Actin expression. The primers used for MIP-2 were (Fwd: CCCAGACAGAAGTCATAGCCAC, Rev: GCCTTGCCTTTGTTTCAGTATC) and B-Actin (Fwd: CACCACACCTTCTACAATGA, Rev: GTCTCAAACATGATCTGGGT). MIP-2 ELISA was performed using a commercially available kit accordingly to manufacturer's instructions (R&D Systems).

Human lung immunofluorescent microscopy

Lung tissue was infiltrated with 1:1 mixture of Tissue-Tek OCT compound (Sakura) and 30% sucrose, then embedded in OCT, flash frozen and stored at -80C before being cut on a cryostat at

10µm thickness. Sections were briefly air-dried, fixed in 4% PFA, washed, then blocked with 1% BSA in PBS. Primary staining was performed with Alexa Fluor 488 mouse anti-human CD31 (WM59, BioLegend, 10ug/ml), Alexa Fluor 647 anti-human CD14 (HCD14, BioLegend, 10ug/ml), and rabbit anti-human CD16 (ab109223, Abcam, 10ug/ml), secondary staining with Alexa Fluor 568 goat anti-rabbit (ab175471, Abcam, 5ug/ml), and nuclear staining with DAPI 1:10,000 in PBS. Images were acquired on the Nikon A1R microscope at the Northwestern University Center for Advanced Microscopy core facility and processed with Nikon Elements software.

S1 +24h Post-transplant Allograft BAL

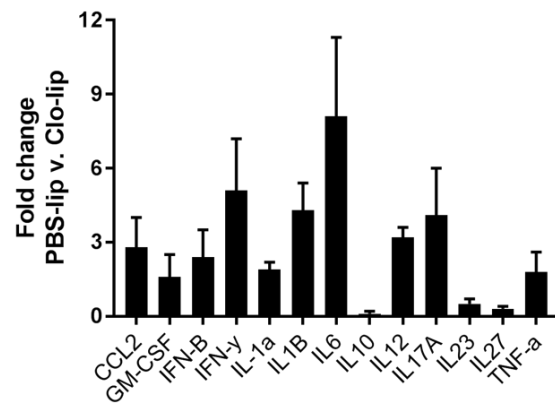


Fig. S1. Cytokine analysis of the lung allograft. Fold-increase of broncho-alveolar lavage (BAL) cytokines in PBS-lip versus Clo-lip treated allografts (n=5 per group). Stastics?

S2

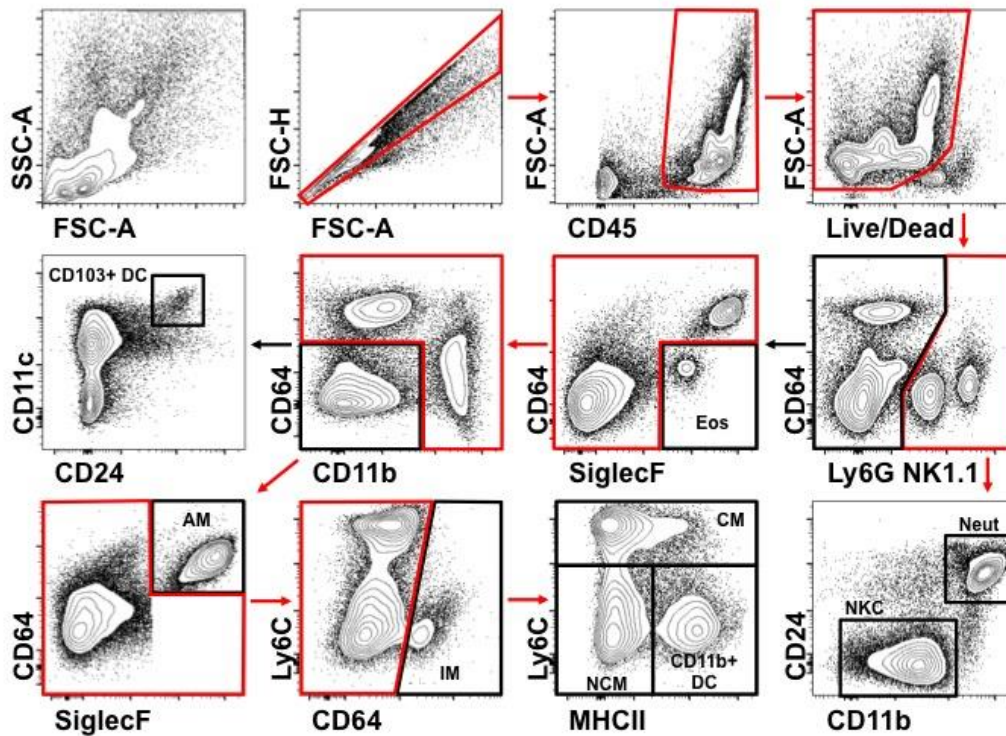


Fig. S2. Representative gating strategy to evaluate the myeloid cell populations in the lungs.

After excluding doublets and dead cells, and including only CD45⁺ cells, neutrophils were identified as Ly6G⁺CD11b⁺CD24⁺, while NK cells (NKC) were identified as NK1.1⁺CD24⁻CD11b^{low/int}. Eosinophils (Eos) were identified as Ly6G^{low}NK1.1⁻SiglecF⁺CD64⁻. After excluding eosinophils, neutrophils, and NK cells, CD103⁺ DC (dendritic cells) were identified as CD11b⁻CD64⁻CD24⁺CD11c⁺ and alveolar macrophages (AM) as CD11b⁻CD64⁺SiglecF⁺. After exclusion of CD11b⁻ cells, interstitial macrophages (IM) were identified as CD64⁺Ly6C^{+/-} and the remaining CD64⁻ cells were either Ly6C^{high}MHCII^{+/-} classical monocytes (CM), Ly6C^{low}MHCII⁻ NCM (NCM), or Ly6C^{low}MHCII⁺ CD11b⁺ DC.

S3

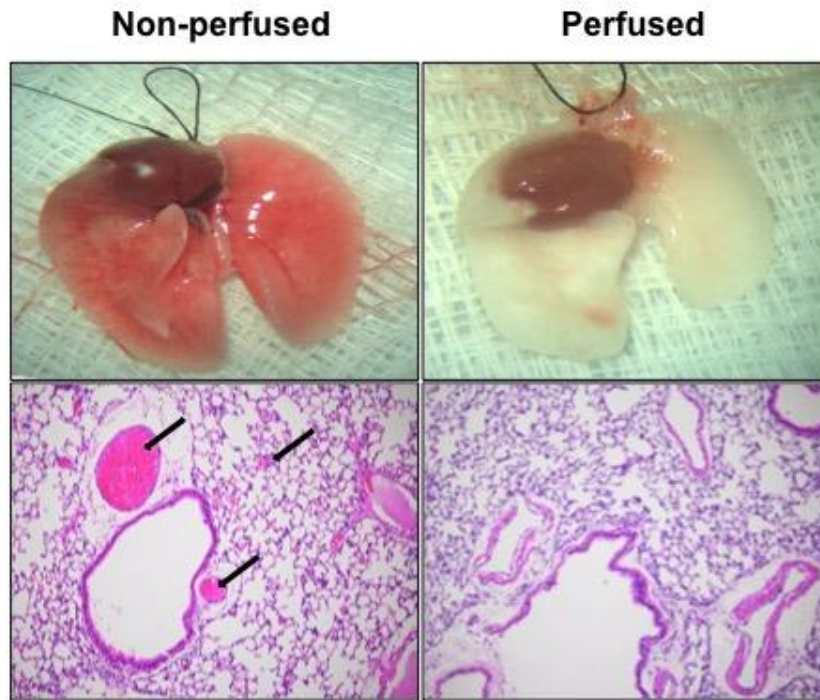


Fig. S3. Perfusion of the heart-lung block. There are no intravascular red blood cells visualized in the perfused whole heart-lung-block: Compared with non-perfused block (left side), the red blood cells (black arrow) were flushed thoroughly in the perfused whole lung block (right side) on both gross and histological evaluation ($\times 200$).

S4

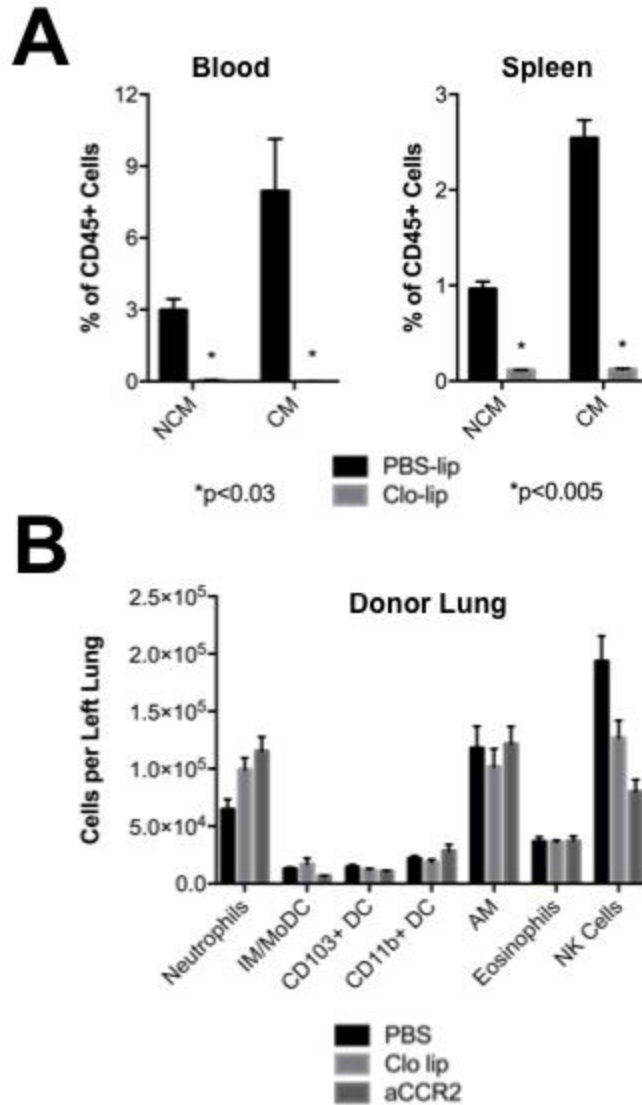


Fig. S4. Effects of monocyte depletion strategies on the donor. (A) Effects of clo-lip treatment on circulating monocytes in the blood and monocytes in the spleen. * $p < 0.005$, by student's t -test with Holm-Sidak adjustment for multiple comparisons, $n = 3$ per group. (B) Effects of clo-lip and anti-CCR2 treatment on non-monocyte lung resident myeloid populations. No comparison by one way ANOVA with Tukey's correction for multiple comparisons met the significance threshold of $p < 0.05$. $n = 3-6$ per group.

S5

+24h Post-transplant Allograft

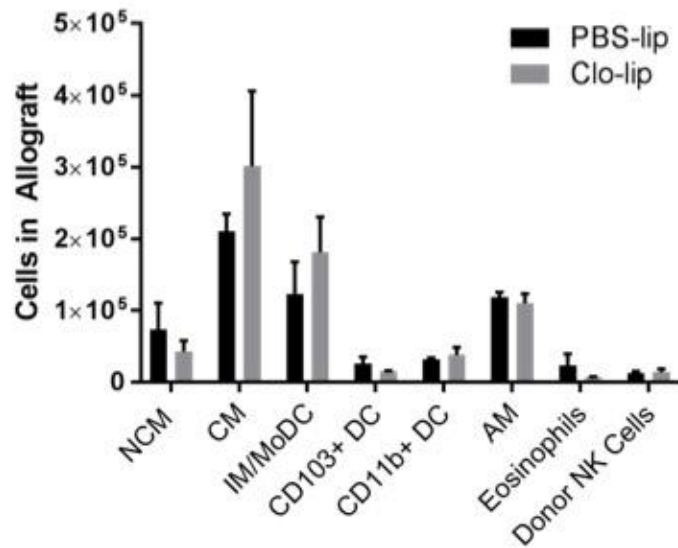


Fig. S5. Effects of donor clo-lip treatment on the 24-hour posttransplant allograft. Effects of donor clo-lip treatment on non-neutrophil myeloid cell types. All comparisons were non-significant by unpaired student's *t*-test with Holm-Sidak adjustment for multiple comparisons. n=5 per group.

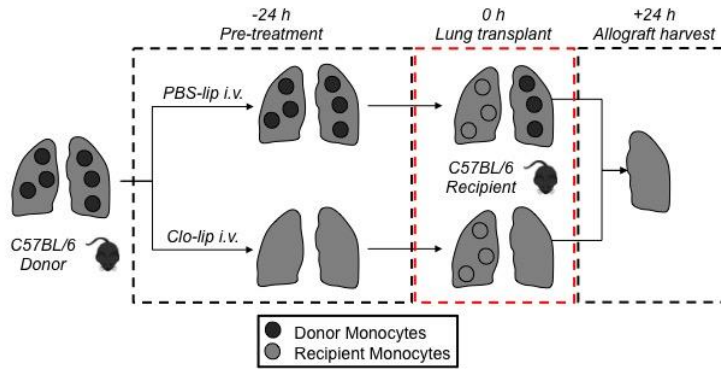
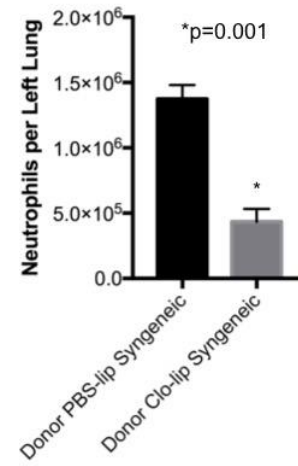
A**B**

Fig. S6. Donor clo-lip treatment abrogates neutrophil influx after syngeneic lung transplant. (A) Experimental design. (B) Effects of donor clo-lip pre-treatment on post-transplant neutrophil infiltration at 24 hours. * $p=0.001$, $n=5$ per group.

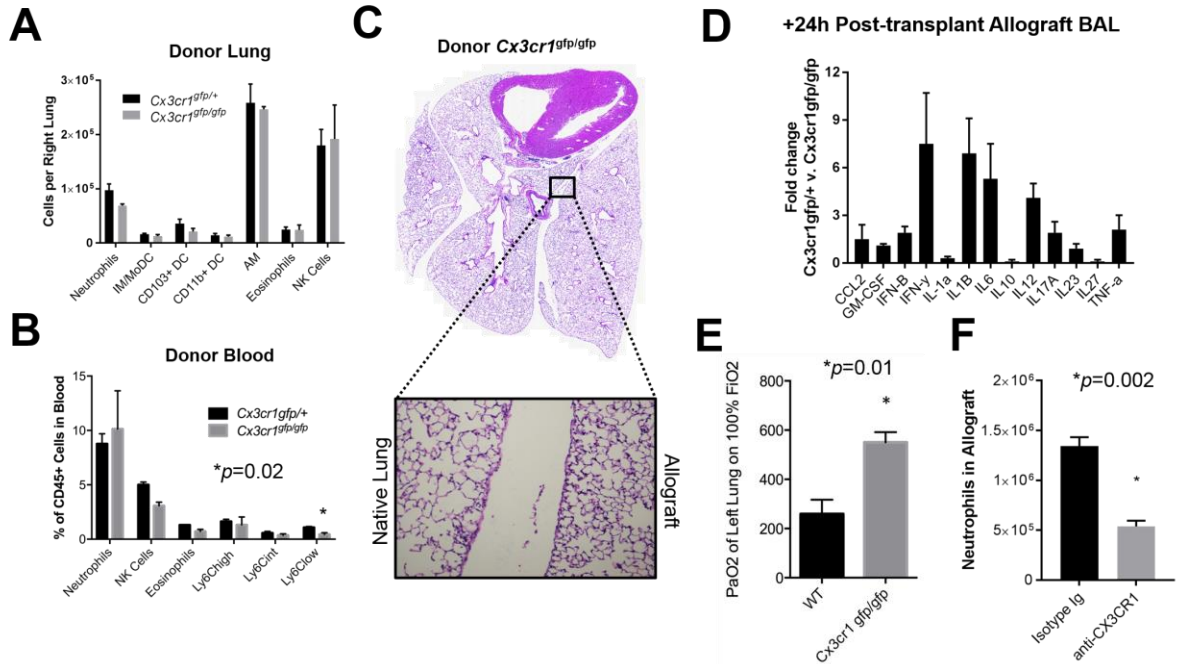


Fig. S7. Effects of CX3CR1 deletion on nonmonocyte cell populations in the lung and blood and on the posttransplant allograft. Effects of CX3CR1 homozygous deletion versus heterozygous control on the (A) non-monocyte myeloid populations in the lung and (B) myeloid populations in the blood. $*p=0.02$, $n=5$ per group. (C) 24 hour post-transplant heart-lung block with inset representing 10X magnification. (D) Effects of CX3CR1 homozygous deletion versus heterozygous control on 24 hour post-transplant allograft BAL cytokines. $n=5$ per group. (E) PaO₂ on 100% FiO₂ of CX3CR1 deficient versus wild type donors. $*p=0.01$, $n=5$ per group. (F) Effects of anti-CX3CR1 blockade on neutrophil infiltration into the allograft at 24 hours post-transplant. $*p=0.002$, $n=5$ per group. All comparisons were made using an unpaired student's *t*-test using a Holm-Sidak adjustment for multiple comparisons where appropriate

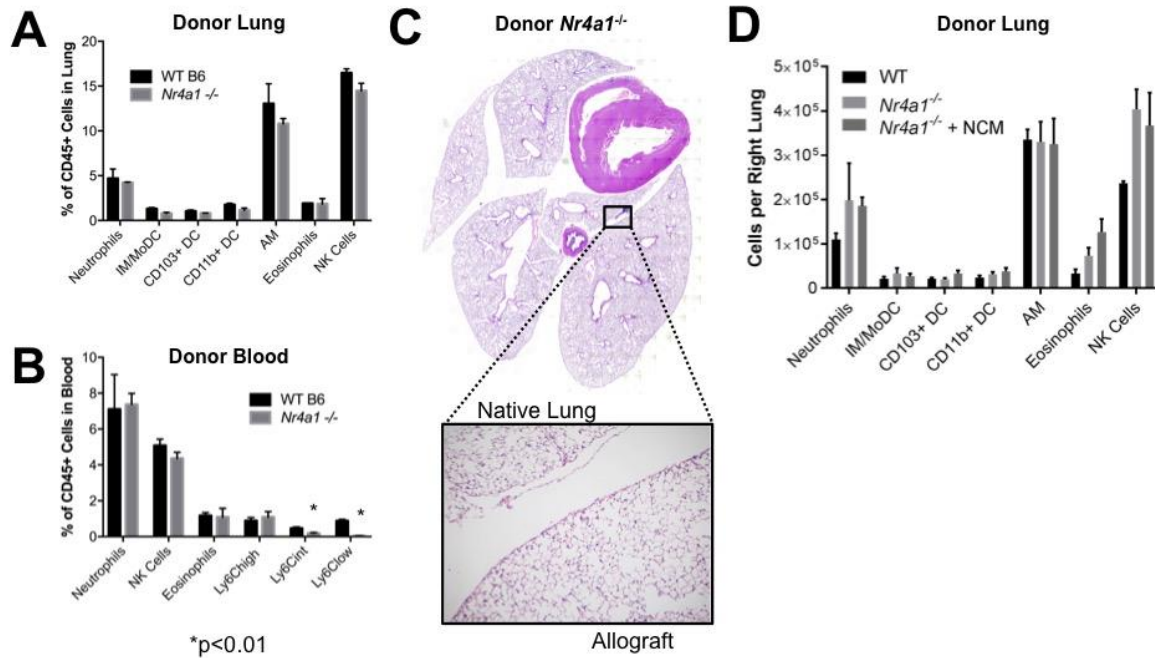


Fig. S8. Effects of NR4A1 deletion on non-monocyte cell populations in the lung and blood and on the posttransplant allograft. Effects of NR4A1 homozygous deletion versus wild type (WT) control on the (A) non-monocyte myeloid populations in the lung and (B) myeloid populations in the blood. * $p=0.0001$, $n=5$ per group. (C) 24 hour post-transplant heart-lung block with inset representing 10X magnification. (D) Effects of NR4A1 deletion and reconstitution of NCM in *Nr4a1*^{-/-} on non-monocyte cell populations in the donor lung. No comparison by one-way ANOVA with Tukey's correction for multiple comparisons met the significance threshold of $p<0.05$.

S9

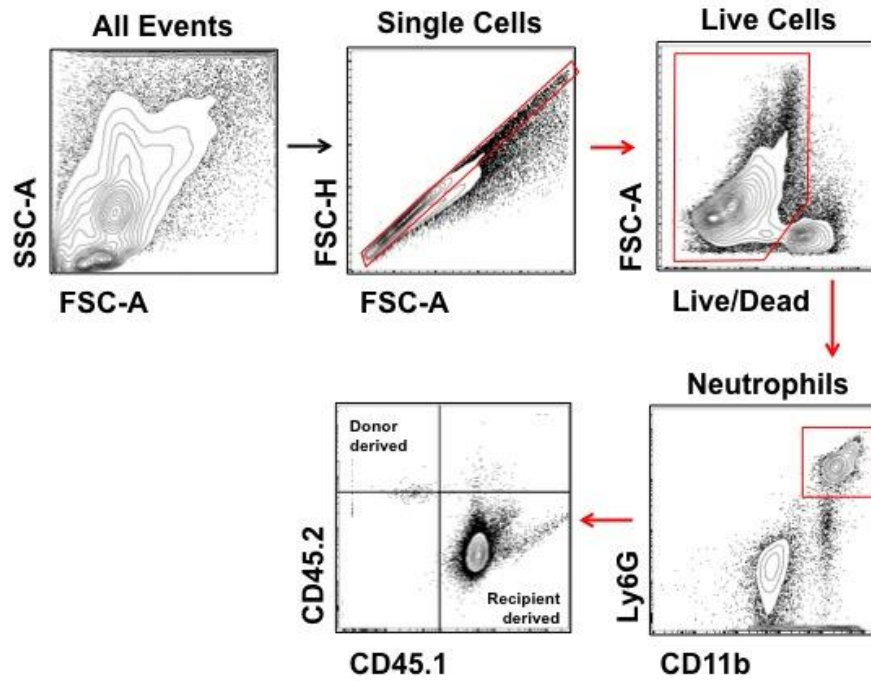


Fig. S9. All neutrophils were of recipient origin after 24 hours of reperfusion in the allograft. Using the orthotopic left lung transplant model from C57BL/6 (CD45.2) to Balb/c (CD45.1), Multicolor flow cytometry analysis in allograft lung at 24 hours after reperfusion.

S10

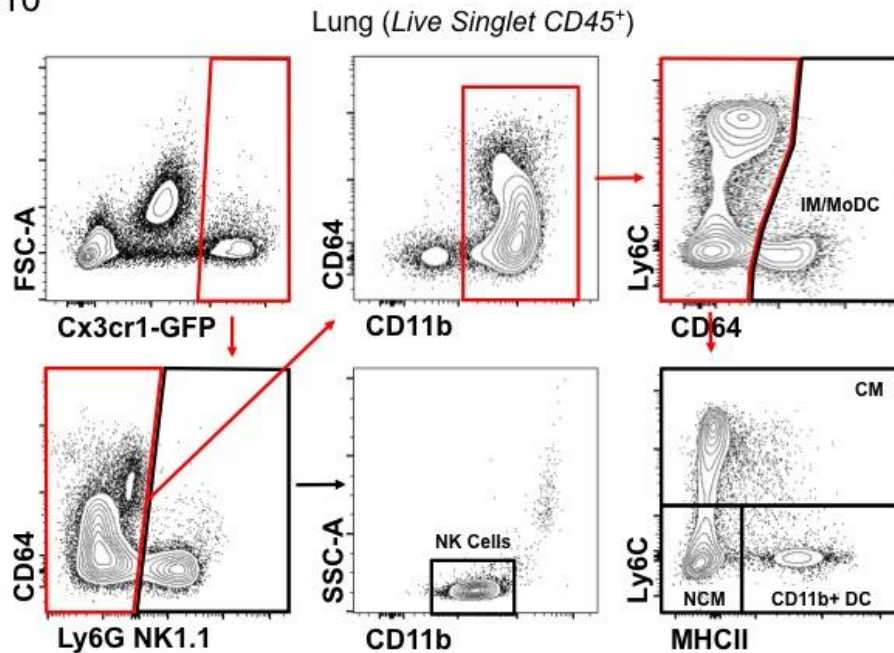


Fig. S10. Representative gating strategy of GFP-expressing cells in the lungs of *Cx3cr1^{gfp/+}* and *Cx3cr1^{gfp/gfp}* mice. After exclusion of doublets and dead cells and including only CD45⁺ cells for analysis, the GFP⁺ population was found to include NK1.1⁺SSC^{low}CD11b^{int} NK cells, Ly6G⁻NK1.1⁻CD11b⁺CD64⁺ interstitial macrophages or monocyte-derived cells (IM/MoDC), and Ly6C^{high}MHCII^{+/-} classical monocytes (CMo), Ly6C^{low}MHCII⁻ NCM (NCMo), and Ly6C^{low}MHCII⁺ CD11b⁺ dendritic cells (DC).

S11

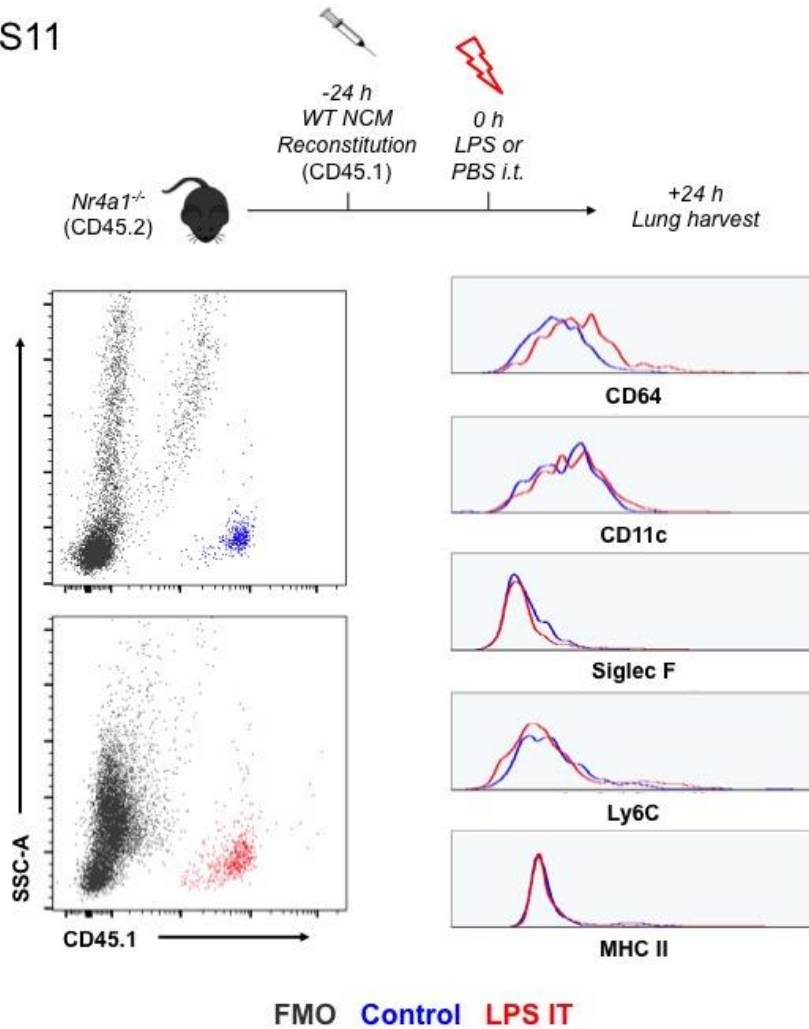


Fig. S11. NCMs do not differentiate upon lipopolysaccharide challenge. Sorted CD45.1 WT NCM were used to reconstitute CD45.2 *Nr4a1*^{-/-} and 24 hours later were challenged with intratracheal lipopolysaccharide. At 24 hours post-LPS challenge, lungs were harvested for flow cytometry. Representative flow plots and histograms are shown (n=3).

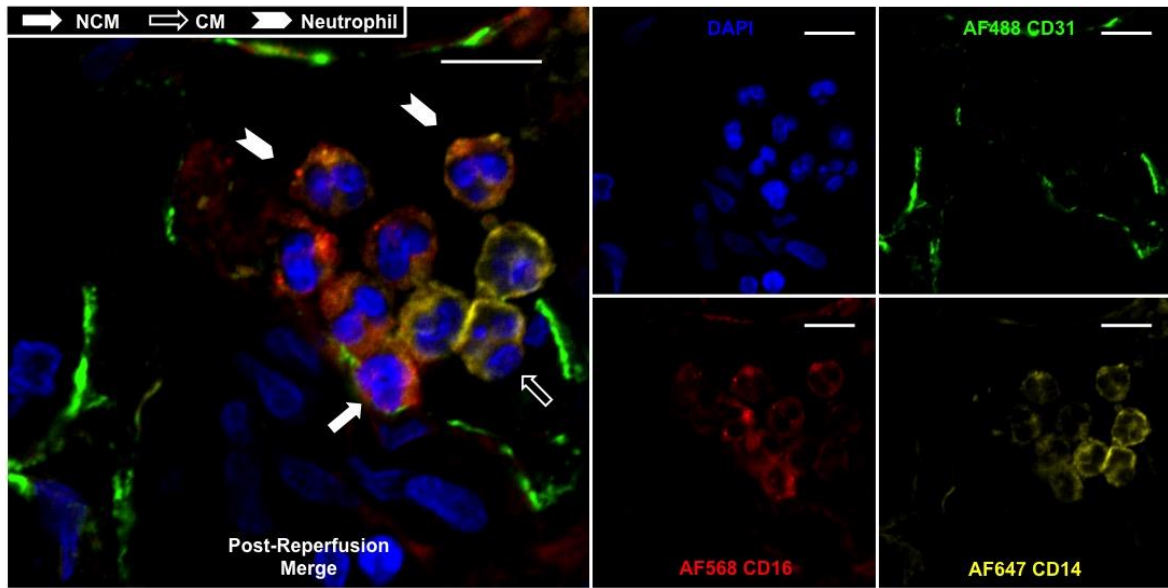


Fig. S12. Immunofluorescence microscopy of human lung biopsy from a patient experiencing PGD. CD16⁺CD14^{dim} NCM (filled white arrows) in the vicinity of clusters of neutrophils (filled white chevrons) and classical monocytes (open arrows) in lung biopsy from a patient experiencing early severe primary graft dysfunction. Green: CD31⁺, Blue: DAPI⁺, Red: CD16⁺, Yellow: CD14⁺. Scale bar represents 10µm.

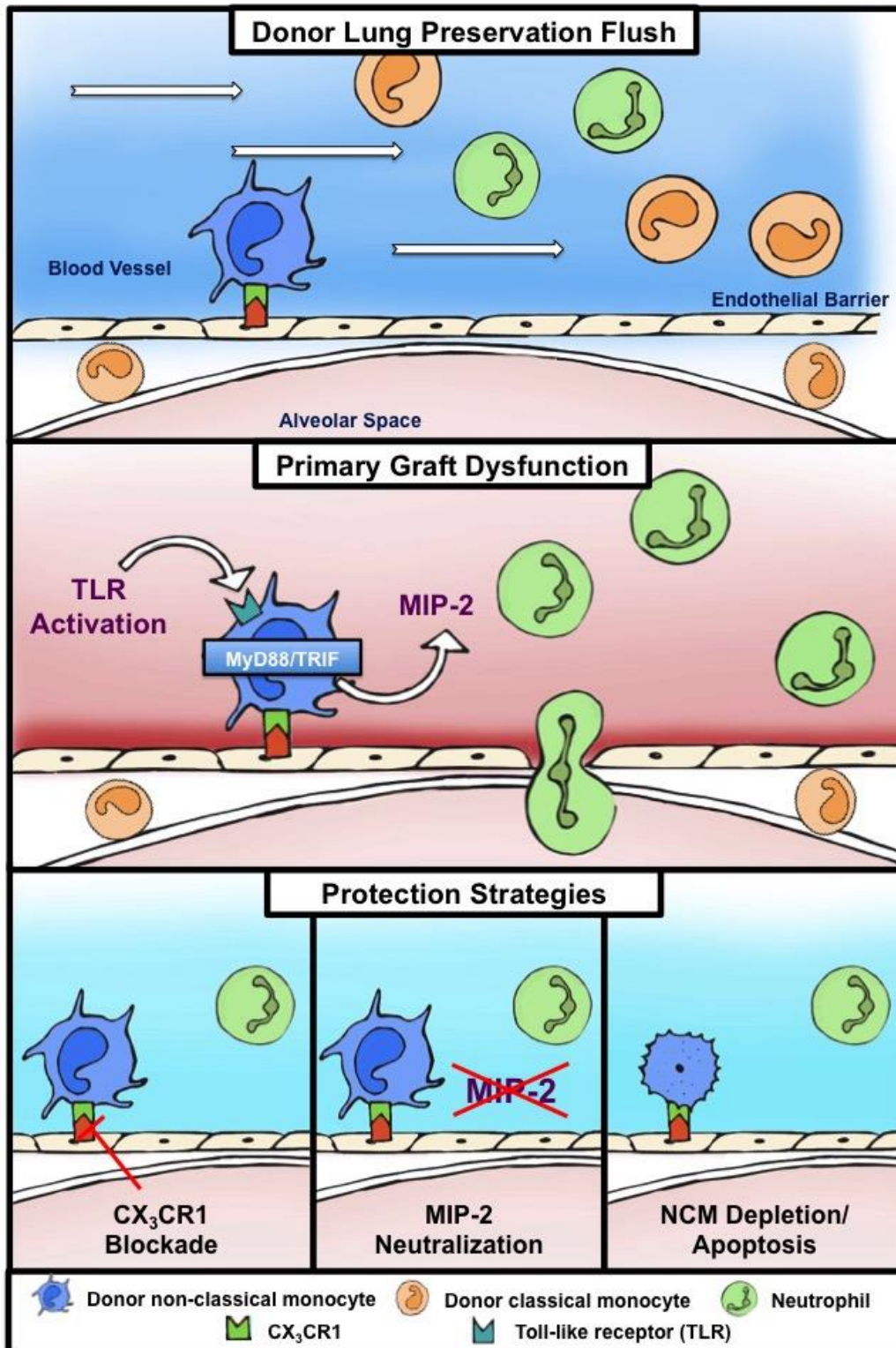


Fig. S13. Schematic to illustrate the role of pulmonary intravascular NCMs in mediating neutrophil infiltration and lung allograft injury. Top panel: At the time of procurement, donor lungs are perfused with a preservative solution to flush all unbound circulating intravascular cells but is unable to remove the NCM bound to the endothelium. Hence, pulmonary intravascular monocytes are retained in the donor lungs. Additionally, interstitial

classical monocytes are retained in the donor lungs. Middle panel: Following reperfusion of the lung allograft, the donor-derived pulmonary intravascular NCM are activated through a Toll-like receptor signaling pathway dependent on MyD88 or TRIF which leads to the production of MIP-2, a key neutrophil chemoattractant, leading to neutrophil influx into the allograft and resulting in primary graft dysfunction. Bottom panel: CX3CR1 blockade, MIP-2 neutralization, or non-classical monocyte depletion represent strategies to ameliorate primary graft dysfunction.

Table S1. Primary data. Provided in Excel.

Movie S1. PBS-lip–treated control mice reveal profound neutrophil infiltration into the lung allograft after reperfusion. Intravital two photon imaging minutes following reperfusion of the lung allograft. The donors were treated with control PBS-liposomes 24 hours prior to transplantation. Recipient are LysM-GFP transgenic mice with neutrophils expressing the GFP protein. Start and end of the movie represent 120 minutes and 150 minutes following reperfusion, respectively.

Movie S2. Intravenous clo-lip treatment of the donors abrogates neutrophil infiltration into the allograft after reperfusion. Intravital two photon imaging following reperfusion of the lung allograft. The donors were treated with intravenous Clo-lip 24 hours prior to transplantation. Recipient are LysM-GFP transgenic mice with neutrophils expressing the GFP protein. Start and end of the movie represent 120 minutes and 150 minutes following reperfusion, respectively.